Intelligent Cockpit for Intelligent Vehicle in Metaverse: A Case Study of Empathetic Auditory Regulation of Human Emotion

Wenbo Li, Lei Wu, Cong Wang, Jiyong Xue, Wen Hu, Shen Li, *Member, IEEE*, Gang Guo, and Dongpu Cao, *Member, IEEE*

***Abstract*—Advances in technologies, such as intelligent connected vehicles and the metaverse are driving the rapid development of automotive intelligent cockpits. From the perspective of the cyber–physical–social system (CPSS), this study proposed the intelligent cockpit composition framework which includes three layers of perception, cognition and decision, and interaction. Meanwhile, we also describe the relationship between the intelligent cockpit framework and the outside environment. The framework can dynamically perceive and understand humans, and provide feedback on the understanding results, which is beneficial to provide a safe, efficient, and enjoyable experience for humans in the intelligent cockpit. In the cognition and decision layers of the proposed framework, we design a case study of active empathetic auditory regulation of driver anger, focusing on improving road traffic safety. We conducted an in-depth interview experiment and designed two auditory regulation materials of active empathy speech and text-to-speech (TTS) speech. Next, 30 participants were recruited, and they completed a total of 240 anger-regulated driving experiments in the straight and obstacle avoidance scenarios. Finally, we quantitatively analyzed and compared the participants' subjective feelings, physiological changes, driving behaviors, and driving risks, as well as validated the driver anger regulation quality of AES and TTS. The proposed research methods results are beneficial to the design of future intelligent cockpit emotion regulation systems, toward a better intelligent cockpit.**

***Index Terms*—Human emotion, human–machine interaction, intelligent cockpit, intelligent vehicle, metaverse.**

Manuscript received 14 November 2022; revised 8 December 2022; accepted 10 December 2022. Date of publication 26 December 2022; date of current version 17 March 2023. This work was supported in part by the China Merchants Testing and Certification Vehicle Technology Research Institute Company, Ltd., under Grant H20220136, and in part by the National Natural Science Foundation of China under Grant 52272420. This article was recommended by Associate Editor F.-Y. Wang. *(Corresponding author: Dongpu Cao.)*

This work involved human subjects or animals in its research. Approval of all ethical and experimental procedures and protocols was granted by the Ethics Committee of the Chongqing University Cancer Hospital, China, under Application No. 2019223, and performed in line with the Declaration of Helsinki.

Wenbo Li, Cong Wang, and Dongpu Cao are with the School of Vehicle and Mobility, Tsinghua University, Beijing 100084, China (e-mail: wenboli@tsinghua.edu.cn; congwang@tsinghua.edu.cn; dp_cao2016@163.com).

Lei Wu, Jiyong Xue, and Gang Guo are with the College of Mechanical and Vehicle Engineering, Chongqing University, Chongqing 400044, China (e-mail: l.wu@cqu.edu.cn; xuejiyong@cqu.edu.cn; guogang@cqu.edu.cn).

Wen Hu is with the College of Mechanical and Vehicle Engineering, Hunan University, Changsha 410082, China (e-mail: huxiaowen@hnu.edu.cn).

Shen Li is with the School of Civil Engineering, Tsinghua University, Beijing 100084, China (e-mail: sli299@tsinghua.edu.cn).

Digital Object Identifier 10.1109/TSMC.2022.3229021

I. Introduction

A. Background and Motivation

THE ADVANCE of intelligent connected vehicles in the past few decades has prompted the transformation of automotive cockpits from traditional cockpits to intelligent cockpits [1], [2], [3]. As a typical cyber–physical–social system (CPSS), the intelligent cockpit is a product that integrates technologies, such as artificial intelligence, new materials, information communication, sensor networks, the Internet of Things, metaverse-related virtual reality, and augmented reality displays [4], [5], [6]. From the perspective of the human–machine–environment, intelligent cockpit should have human–machine integration capability, scenario expansion capability, and network-connected service capability. Human–machine integration capabilities, network-connected service capabilities, and scenario expansion capabilities are the core capabilities of intelligent cockpit to provide services for humans. Three capabilities of human–machine integration, network-connected service, and scenario expansion support each other and jointly promote the improvement of overall service drivers and passengers' ability of the intelligent cockpit. With the rapid development of the above three capabilities, the intelligent cockpit will evolve into a human-centered intelligent mobile space in the future [7].

The human–machine integration capability represents the ability of the intelligent cockpit to perceive, understand, and make corresponding decisions to serve the drivers and passengers [8], [9]. It is the core technology of the intelligent cockpit service humans in cabin. The application of technologies, such as DMS, AR-HUD, smart surfaces, and multimodal interaction has promoted the progress of human–machine integration capabilities, enabling the intelligent cockpit to serve humans more "humanized." The network-connected service capability represents the ability of the intelligent cockpit to provide rich functions and services for drivers and passengers. The application of network-connected technologies, such as 5G, information and communication technology, cloud services, and over-the-air technology has promoted the continuous upgrading of intelligent cockpit network-connected capability to the Internet of Everything, and the functional applications and service content provided by the intelligent cockpit for humans are becoming more and more abundant. The scenario expansion capability represents the ability to expand the boundaries of the intelligent cockpit service drivers and passengers (from the driver to the passengers, from inside the cabin to outside the cabin). The interconnection of smartphones, smart bracelets, and smart homes with intelligent cockpits continuously expands the scenario boundaries of intelligent cockpit service humans. The intelligent cockpit will be able to meet the needs of humans in various travel scenarios, such as entertainment, socializing, and working.

Although the intelligent cockpit is an important space for the human–vehicle relationship evolving from a driving tool to an intimate partner, the future intelligent cockpit still needs to answer a challenging question, that is how to take advantage of the continuous development of innovative technologies to allow the intelligent cockpit to provide people with precise functionalities and services for the safe, efficient, and enjoyable experience [7], [10]. To address this problem, under the CPSS framework, we propose an intelligent cockpit composition framework, discussing the compositions of the intelligent cockpit and the technologies each composition should have (see the discussion in Section I-A for details). Meanwhile, in this article, to further describe the application potential of this framework, we also describe a case study of driver angry emotion regulation under the framework.

B. Intelligent Cockpit Framework in Metaverse

Fig. 1 highlights the composition framework of the intelligent cockpit, and the relationship between the intelligent cockpit and the outside environment [11]. As mentioned above, the intelligent cockpit is a mobile interactive space with humans as the core. With the assistance of the in-cabin technology, the intelligent cockpit can dynamically perceive and understand humans and give feedback on the understanding results. Therefore, in our framework, the intelligent cockpit contains three layers: 1) perception; 2) cognition and decision; and 3) interaction. In addition, the network-connection property of the intelligent cockpit allows it to communicate with the environment outside the cabin to provide humans with more comprehensive services. Therefore, we also present the interaction between the outside environment of the intelligent cockpit and the intelligent cockpit. The proposed framework will dynamically record the in-cabin humans and the outside environment for real-time perception, cognition and decision, and interaction, providing a safer, more efficient, and enjoyable experience for humans. Each layer of the intelligent cockpit is explained in more detail in the following.

1) Intelligent Cockpit Perception: The perception layer can use various sensors to perceive humans in the cockpit and environmental information outside the cockpit, so as to obtain multimodal information, and then send the perceived information to the cognition and decision layers. The perception layer includes two modules of various sensors and multimodal information extraction. In the various sensor module, the intelligent cockpit can use visual sensors [12] (in-cabin cameras, outward cameras, etc.), auditory sensors [13] (microphones, etc.), tactile sensors [14] (smart interactive surfaces, smart textiles, steering wheel, dashboard, screen, seat, etc.), olfactory sensors (digital olfaction technology, etc.), physiological sensors (EMG [15], EEG [16], ECG, EOG, IMU, wearable devices [17], etc.), and driving sensors (steering wheel, throttle, brake, etc.) arranged inside and outside the cabin to obtain corresponding multimodal information. For example, it can obtain visual information, such as facial expression, head posture, body posture, hand gesture, in-cabin scenario, and outward scenarios; auditory information, such as linguistic speech and nonlinguistic speech; tactile information, such as finger/hand/body pressure; olfactory information such as smells in-cabin; physiological information, such as heart, electrodermal activity, skin temperature, respiration, brain activity, and muscle activity; driving behavior information, such as steering and speeding.

2) Intelligent Cockpit Cognition and Decision: The cognition and decision layer uses the multimodal data transmitted by the perception layer to detect the human behavior and state in the cabin [18], further predict the human behavior and state [19], [20], complete the generation of assessment and decision strategies [21], and finally transmit the assessment and strategies results to the interaction layer. The multimodal data includes human data, dynamic in-cabin scenario data, and extra-cabin scenario data. The human behavior and state detection stage are mainly to identify human emotions, fatigue [22], distraction [23], intention [24], and other behaviors and states [25]. The corresponding intelligent cockpit can also predict human emotion, fatigue, distraction, intention, and other states. The assessment and strategies stage includes dynamic cockpit scenario adaptive strategies [26], human behavior intervention strategies, human state regulation strategies, and customized service strategies. It should be noted that at each stage of cockpit cognition and decision, history data, such as personality and personal habit records, personalized preference and customized service, health condition history, etc., stored in cyberspace provides help [27].

3) Intelligent Cockpit Interaction: With the output strategy guidance of the cognition and decision layer, the interaction layer can provide service for the human in the cabin using a variety of interaction methods, and can also interact with the environment outside the cabin. The interaction in the cabin is divided into unimodal interaction and multimodal interaction. Unimodal interaction consists of visual interaction [28] (visual intervention, ambient light, HUD, AR, 3-D display, etc.), auditory interaction (adaptive music, empathetic speech, the voice of assistant, etc.), tactile interaction [29] (vibrotactile, temperature control, etc.), and olfactory interaction (peppermint, vanilla, rose, etc.). Multimodal interaction [30] combines different unimodal interaction methods, such as interior adaptations, empathetic agents, and customized service [31]. Using technologies, such as information communication and vehicle exterior surfaces, the intelligent cockpit can also interact with other vehicles [32], pedestrians, infrastructure, and smart homes in the outside environment.

The proposed framework is the overall architecture diagram and technical framework for realizing the intelligent cockpit. The framework is the specific representation of the future intelligent cockpit human–machine integration capabilities, network-connected service capabilities, and scenario

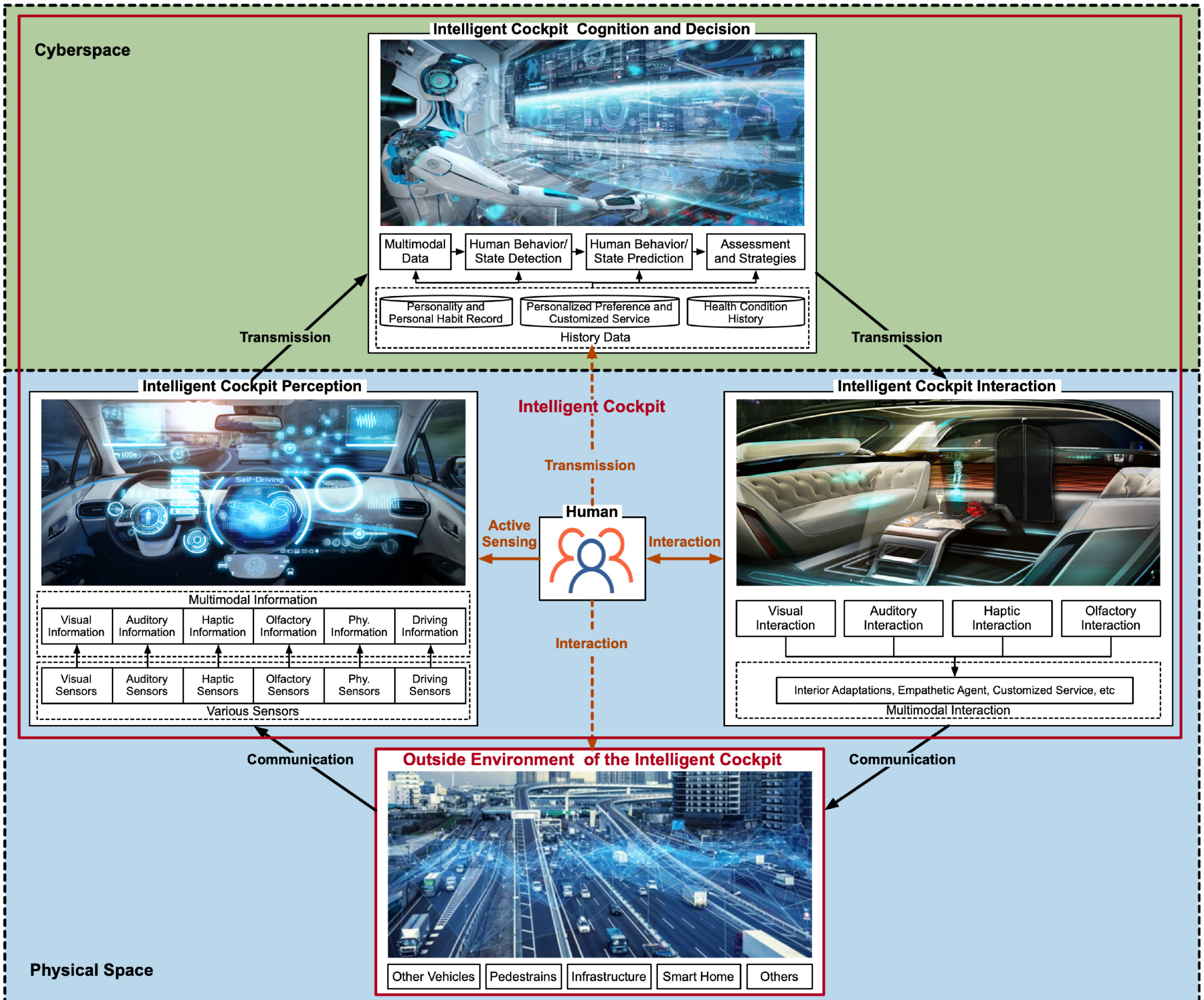

Fig. 1. Composition framework of the intelligent cockpit, and the relationship between the intelligent cockpit and the outside environment

expansion capabilities (for example, the human–machine integration capability are reflected in the intelligent cockpit perception, cognition and decision making, interaction parts; the information transmission and communication of the intelligent cockpit in the physical space and cyberspace reflects the network-connected service capability; the interaction between the intelligent cockpit and the smart home, infrastructure, etc. in the external environment reflects the scenario expansion capability). The continuous improvement of human–machine integration capabilities, scenarios expansion capabilities, and network-connected service capabilities will promote the overall advancement of the proposed technical framework's ability to serve humans in the cabin.

One of the potential applications of the framework described above is that the dynamic cooperation of the three layers of the intelligent cockpit can improve traffic safety, especially for addressing the increased driving risk caused by extreme driver emotions. Extreme driver emotions, such as anger, have long been one of the leading causes of road accidents worldwide [33]. In the intelligent cockpit, the perception, cognition, and decision of the driver's anger, as well as the regulation of the driver's anger through different interaction methods are an effective way to reduce the driving risk caused by anger and thereby improve road traffic safety. Benefiting from the rapid development of technologies, such as artificial intelligence, existing research has made great progress in driver anger detection and different interaction technologies development [34], [35], [36]. However, few studies have focused on what decisions the intelligent cockpit should make after recognizing anger, and generating corresponding strategies to regulate driver anger effectively. To address this issue, in this work, we propose a research method for driver anger regulation using active empathetic speech (AES) and conduct experiments to verify the effectiveness of different speech regulation strategies.

C. Contributions and Organization

The contributions of this article can be summarized as follows.

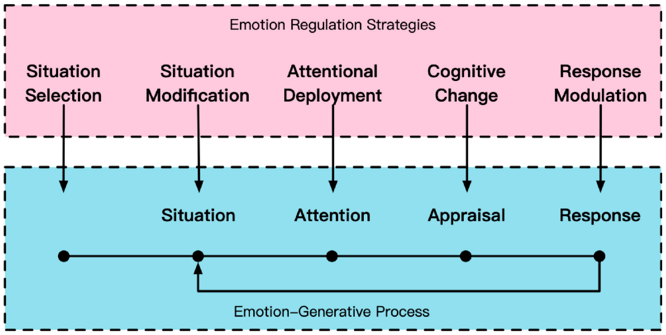

Fig. 2. Process model of emotion regulation [37].

1) From the perspective of CPSS, the intelligent cockpit composition framework for connected automated driving in the metaverse is proposed. The framework includes three layers of perception, cognition and decision, and interaction, and we also discussed the typical technologies in each layer. Meanwhile, we also describe the relationship between the intelligent cockpit framework and the outside environment. The framework can dynamically perceive and understand humans, and provide feedback on the understanding results, providing a safe, efficient, and pleasant experience for humans in the intelligent cockpit.
2) In the cognition and decision layers of the proposed framework, we design a case study of active empathetic auditory regulation of driver anger, focusing on improving road traffic safety. We conducted an in-depth interview experiment and designed two auditory regulation materials of AES and text-to-speech (TTS). Next, 30 participants were recruited, and they completed a total of 240 anger-regulated driving experiments in the straight and obstacle avoidance scenarios.
3) Finally, we quantitatively analyzed and compared the participants' subjective feelings, physiological changes, driving behaviors, and driving risks, and finally validated the driver anger regulation quality of AES and TTS.

This study is organized as follows. First, related work on driver emotion regulation is discussed in Section II. In Section III, a detailed introduction to auditory-based driver anger regulation experiments and the selection of auditory regulation materials is discussed. In Section IV, the experimental results are analyzed and discussed. Finally, the conclusion is made in Section V.

II. Related Work

A. Emotion Regulation Model

This section describes the process model for emotion regulation [37]. The process model of emotion regulation is based on the emotion modality model and takes each step in the emotion generation process described by the modality model as a potential regulation target. Fig. 2 presents the process model, which highlights five points at which individuals can regulate their emotions. These five points represent the main components: 1) situation selection; 2) situation modification; 3) attentional deployment; 4) cognitive change; and 5) response modulation [37]. Fig. 2 shows that emotion regulation plays an important role in the process of emotion generation. The movement from left to right in Fig. 2 represents the movement of time: a specific situation is selected, modified, focused, appraised, and a specific set of emotional responses is generated. At the same time, the generation of emotion is a continuous dynamic process, and this dynamic aspect is represented by the feedback arrow in Fig. 2, from the emotional response back to the situation.

For emotion regulation in driving, due to the unpredictability of the driving environment, drivers are often unable to choose routes with low traffic flow and smooth flow (situation selection or situation modification), so as to avoid the negative impact of traffic jams on emotions. Furthermore, due to the complexity of the driving task, cognitive change, and response modulation may increase the driver's cognitive effort and driving workload and have an impact on the driving task. Therefore, under the premise of avoiding distraction, attention deployment may be an effective method for driver emotion regulation.

B. Auditory Emotion Regulation in Driving

Compared to visual regulation, auditory emotion regulation reduces mental, and visual distraction [38]. Therefore, many studies on auditory emotion regulation have been carried out, including adaptive music, auditory intervention, and empathetic speech. Many studies envisage the application of adaptive music in the driving environment to regulate the driver's emotions [39], [40], [41]. Studies have indicated that recommending calm music to drivers in a high arousal state could help them calm down and will affect driver's emotional states and driving behavior in the long run [42], [43], [44]. However, other studies have pointed out that although music affected driving behavior and reaction times, it had no significant effect on subjective emotion levels [45]. A typical form of auditory intervention is to instruct the driver to perform breathing exercises. Paredes et al. [46] conducted breathing interventions to improve alertness and calmed down the aroused drivers through slow breathing instructions. Zepf et al. [47] also investigated auditory breathing interventions for drivers to relieve stress, and they found that conscious intervention more effectively reduced the breathing rate but also increased the number of driving mistakes.

Empathetic speech requires empathetic adaptation of the in-vehicle voice agent's speech output to adapt to the emotional state of drivers and passengers in the driving environment. Studies on empathetic speech revealed that the matched speech arousal level could have a positive impact on driving behavior and the frequency of interactions [48]. A study by Braun et al. [49] showed that empathetic speech was not only liked by drivers but also could decrease the impact of sadness and anger on driving. Empathetic speech may be a suitable method to regulate the driver's negative emotions. However, the above studies all worked with prototypical interactions. A clear description of empathy in voice interactions may require further research [50].

C. Characteristics of Empathetic Speech Emotion Regulation

Previous studies on the characteristics of empathetic speech include voice age, voice familiarity, voice content, and voice expression style. For the voice age, Jonsson's study showed that the use of a young voice significantly improved the drivers' driving performance than that of an older voice [51], and it is found that male voices are better at expressing instructive and technical signals, whereas female voices are better at conveying emotional and caring information [52]. Therefore, in this study, we chose a young female voice as the voice age characteristic. In terms of voice familiarity, previous studies revealed that using familiar sounds positively affected drivers' driving feelings and driving performance (avoiding traffic accidents, abiding by traffic rules and lane offset) than using unfamiliar sounds [53]. In addition, some drivers proposed that individualized voice warnings, such as recording the voices of relatives, friends, or themselves, can help reduce driving anger [54]. In this study, we selected familiar speech prerecorded by friends and, at the same time, used unfamiliar TTS synthesized speech for comparison.

The voice content characteristic can cause emotional changes in drivers. The findings of Jonsson's study revealed that environment-related voice content worked best, and drivers felt most relaxed under such content [55]. Li et al. compared the effects of positive comments and negative comments on drivers in anger. The results showed that positive and negative comments could help drivers feel less angry and improve driving performance. Furthermore, positive comments containing descriptions of the driving environment and the driver were more effective than negative comments [56]. In this study, we further verified the speech content in addition to the environment. For the voice expression style, Jeon et al. compared the effects of situation awareness warning in a notification style and emotion regulation warning in a command style on angry drivers. The findings revealed that the two styles of speech-based warnings lowered drivers' irritation and perceived burden while simultaneously improving their driving concentration and performance [57]. Therefore, we selected the notification style to remind the driver.

III. Emotion Regulation Experiment

A. Participants

A total of 30 participants (20 males and 10 females) were recruited for this experiment. Participants have ranged in age from 19 to 27 ($M = 23.23$ years old and SD = 1.65). All of the participants were in possession of a valid driver's license and had at least one year of driving experience ($M = 2.7$ years and SD = 1.58). All participants reported that their eyesight and hearing were normal or corrected to normal. All participants received guidance on experimental procedures and signed informed consent before participating in the experiment. Participants had the option to terminate the experiment at any time if they were uncomfortable.

B. Material and Apparatus

1) Anger Induction Material: Previous research has found that video clips are an effective method for driver emotion induction [33], [36], [58]. Therefore, selected video clips were played to stimulate the participants' anger. From the PPB_Emo dataset [10], we selected three video clips recorded to be used to elicit participants' anger. For example, others keep the high beam on while meeting the car, which affects the vision. These video–audio clips have already been confirmed to be reliable and can trigger drivers' anger. Each video–audio clip lasts from 10–30 s.

2) Regulation Success Scale: The following question was employed to assess the participants' perceived success in emotion regulation: "Overall, on a 10-point Likert scale (1 = "not at all successful" and 10 = "extremely successful"), how successful do you think you are at altering your emotions" [59].

3) Differential Emotions Scale: The differential emotions scale (DES) [33] was employed to measure whether each participant experienced the target emotion (anger or neutral).

4) Driving Simulator: Emotion regulation experiments were performed on a driving simulator (RDS2000, Real-Time Technology, Ann Arbor, USA) with a semi-vehicle body, steering wheel, adjustable car seat, automatic transmission, gas, and a brake pedal. The driving behavior data of each participant was collected by the driving simulator, including lateral and longitudinal control data (velocity, acceleration, gas position, braking force, steering wheel angle, etc.). Besides, in this study, selected auditory regulation materials were also played through the driving simulator's two implanted speakers.

5) Electroencephalogram Device: A wireless Electroencephalogram (EEG) device (EnobioNE, Neuroelectrics, Barcelona, Spain) was employed to collect the participant's brain activity. As shown in Fig. 3, this EEG device has 32 channels and contacts the participant's brain through 32 dry electrodes. EEG signals were displayed through the NIC2 software, which can acquire and processes the signals. Through the NIC2 software, alpha bands (8–13 Hz) of all electrode positions were sent to the computer. Notably, the brain activity and driving behavior data of each participant were synchronously stored.

C. Driving Scenarios and Procedure

1) Driving Scenarios: As shown in Fig. 4(a), two road scenarios simulating suburban highways were created on the simulator, one was a practice scenario and the other was an experimental scenario. Both scenarios simulate common trees, buildings road signs, and vehicles in real-world driving environments. The practice scenario was intended to assist participants in becoming acquainted with the driving simulator before the formal experiment. The practice scenario was a straight road with a length of 2 km. According to the road signs (80–40–60 km/h) in the scenario, participants drove on two-way four lanes at different speeds. The experimental scenario used in the formal experiment was shown in Fig. 2, which contained two traffic events: 1) straight driving and 2) obstacle avoidance. Each participant was required to finish driving tasks in the straight driving event at a speed of 80 km/h, and in the obstacle avoidance event at a speed of 60 km/h.

TABLE I
DESCRIPTIONS OF THE FOUR DRIVING CONDITIONS

Driving Condition	Descriptions
AES-RD	Active empathetic speech emotion regulation driving. The participant was induced anger by video-audio clips. He/she was regulated with empathetic speech from their friends
TTS-RD	TTS emotion regulation driving. The participant was induced anger by video-audio clips. He/she was regulated with TTS speech from a stranger
AD	Angry driving. The participant was induced anger by video-audio clips. No emotion regulation.
ND	Neutral driving. The participant was induced neutral by video-audio clips. No emotion regulation.

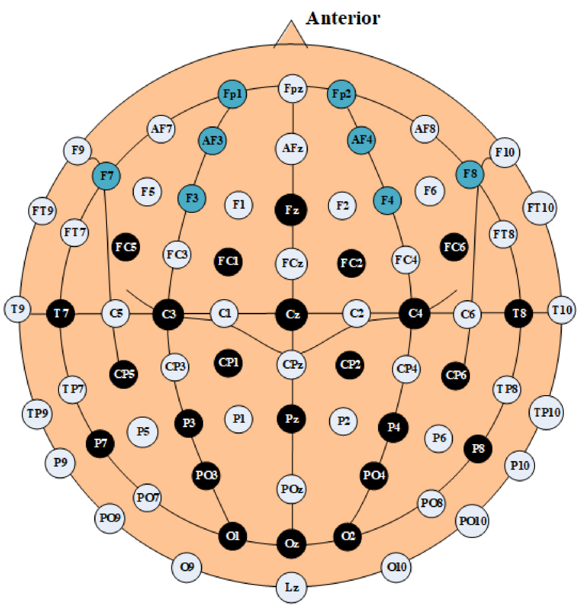

Fig. 3. Selected electrodes of the EEG.

2) Procedure: Before the experiment, the participants were briefed on the contents of the experiment. After signing an informed consent form and completing a demographic questionnaire, participants entered the driving simulator and modified the seat such that the steering wheel and pedals could be operated comfortably. Then, participants wore EEG caps and the experimenter completed the calibration of the EEG signals. Next, each participant had about 10 min of practice driving. After the practice driving, participants were asked to randomly look an anger-inducing video–audio clip and participants reported their experiencing emotions by DES scale. Then, each participant finished four 2-km long formal drives under four driving conditions, including AES-regulation driving (AES-RD), TTS-regulation driving (TTS-RD), angry driving (AD), and neutral driving (ND) with a 5-min break between each drive, more details in Table I. After each drive, participants filled out the regulation success scale. Each participant's experiment time lasted about 1 h. The data collection setup and the experimental procedure are shown in Fig. 4(b) and (c).

D. Auditory Regulation Content

1) In-Depth Interview: Empathetic speech has been shown to be effective in improving drivers' negative emotions. Therefore, in this study, we used the empathetic speech as auditory regulation material. To select the content of driver anger-auditory regulation material, we conducted in-depth interviews with eight participants. The interviews were based on the interview guide method. Participants answered an open-ended question ("what kind of reminder/feedback would you most like the car to give you when you're angry while driving?"). During the answering process, the participants were instructed to use their own words to describe the reminders they would like the intelligent vehicle to give (for example, to answer "I hope the car will encourage me at this time, such as you drive well."). The interview time for each participant was around 20 min.

2) Regulation Material Content: The interview results showed that the reminder of the road environment could divert the driver's attention well to improve their negative emotional state. In addition, the participants felt a positive emotion when they received praise or emotional support from friends or family, as positive comments helped build the driver's confidence, which may reduce some negative effects of anger. Therefore, in this study, we used the emotion regulation strategy based on attention deployment. Combined with previous research [56], [57], a reminder style tells the driver about the current road environment (e.g., "there is an obstacle ahead, we need to be careful"). Moreover, the voice content uses positive comments (e.g., "you're driving well") to praise the driver. The contents of the auditory regulation materials adopted in this study are shown in Table II. Notably, to better verify the regulation quality of empathetic speech, we also selected TTS sound as the baseline for comparison. For TTS voice, we used the iFLYTEK platform (https://www.xfyun.cn/services/online_tts) to generate two speech files with a young female voice. For the empathetic speech, we recorded two voice clips of participants' female friends in advance. In both types, the content of the speech clips is exactly the same (see Table II), and the average duration of voice clips is approximately 4 s.

IV. RESULT AND DISCUSSION

A. Data Analysis Indicators and Method

In this study, a total of 30 participants finished the experiment. Each participant experience four driving conditions which are described in Table I. The independent variable of the experiment was driving conditions and the dependent variables were subjective feelings (subjective emotional scores and regulation success ratings), physiological changes, and driving behavior.

(a) (b) (c)

Fig. 4. Experimental setup: (a) experiment scenarios; (b) data collection setup; and (c) experimental procedure.

TABLE II
AUDITORY EMOTION REGULATION SCHEMES AND CORRESPONDING SCENARIOS

Scenarios	Straight Driving Phase	Obstacle Avoidance Phase
Regulation Time	After getting the engine started	After a damaged vehicle appeared
Empathetic Speech	The road is beautiful. Don't be angry. You are a good driver.	There is an obstacle ahead, and we need to be careful. Your driving is excellent.
TTS Speech	The road is beautiful. Don't be angry. You are a good driver.	There is an obstacle ahead, and we need to be careful. Your driving is excellent.

For subjective feelings, we used DES and regulation success scale scores to measure subjective emotion scores and regulation success rates, respectively. For physiological changes, previous studies have shown that asymmetric activity in the prefrontal cortex is crucial for emotion control, and asymmetry in frontal activity might be a physiological sign of anger [33]. In this work, we chose frontal brain electrical asymmetry as a physiological indicator of anger regulation quality. On the left and right sides of the prefrontal lobe, four pairs of electrodes were picked: 1) F3-F4; 2) F7-F8; 3) AF4-AF3; and 4) Fp1-Fp2. According to previous studies [60], safe drivers rarely accelerate or brake suddenly. Therefore, the driving behavior indicators included average speed, mean gas position, and mean pedal force. Further, we also analyzed the driving risk of four driving conditions.

SPSS software was used for statistical analysis. The influence of various driving conditions on subjective emotion scores, physiological data, driving behaviors, and driving risk were evaluated using a one-way ANOVA.

B. Subjective Feelings

1) Manipulation Checks: Participants experienced three anger inductions under four drives. Drivers' emotions were checked through two self-report questionnaires (before-experiment and post-experiment).

We identified whether anger induction was successful: when participants reported that their anger rating was 6 or higher, we considered that the anger induction was successful. The results showed that the experiment successfully induced anger in at least 25 participants.

Fig. 5 shows the change of participants' anger rating scores on the Likert scale, from 1 (not angry at all) to 9 (very angry). One-way ANOVA showed that the ND condition

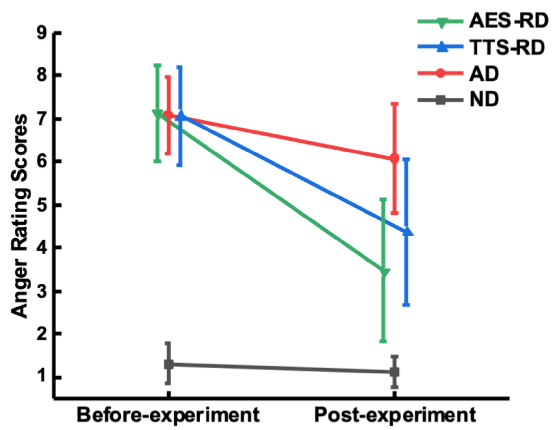

Fig. 5. Anger rating scores across three timings. Error bars indicate the standard error of the mean.

TABLE III
RESULTS OF ANGER RATING SCORES FOR FOUR DRIVING CONDITIONS

Driving conditions	F	η_p^2	Mean (SD)		Cohen's d
			Before-experiment	Post-experiment	d
AES-RD	103.571	0.641	7.13 (1.11)	3.47 (1.63)	4.587***
TTS-RD	52.488	0.475	7.07 (1.14)	4.37 (1.69)	3.078***
AD	12.476	0.177	7.07 (0.87)	6.07 (1.28)	2.069***
ND	2.474	0.041	1.30 (0.47)	1.13 (0.35)	0.735

d Before-experiment verus Post-experiment; *p<.05, **p<.01, ***p<.001.

($F(1, 59) = 2.474, p = 0.121$, and $\eta_p^2 = 0.041$) had no significant difference. But the AD condition ($F(1, 59) = 12.476, p = 0.001$, and $\eta_p^2 = 0.177$), the TTS-RD condition ($F(1, 59) = 52.488, p < 0.001$, and $\eta_p^2 = 0.475$) and the AES-RD condition ($F(1, 59) = 103.571, p < 0.001$, and $\eta_p^2 = 0.641$) reported significant difference (see Table III).

A paired-samples t-test was performed on the two rating scores under the AD condition. It was found that the anger rating scores after the experiment ($M = 6.07$ and $SD = 1.28$) were significantly lower than those before the experiment ($M = 7.07$ and $SD = 0.87$), $p < 0.001$, and $d = 2.069$. Paired samples t-tests were conducted on the two anger rating scores under the TTS-RD condition. The results showed that the post-experiment anger scores ($M = 4.37$ and $SD = 1.69$) was significantly lower than the preexperiment scores ($M = 7.07$ and $SD = 1.14$), $p < 0.001$ and $d = 3.078$. Paired samples t-tests were also performed on the two rating scores under the AES-RD condition. The results indicated that the anger rating scores after the experiment ($M = 3.47$ and $SD = 1.63$) were significantly lower than those before the experiment ($M = 7.13$ and $SD = 1.11$), $p < 0.001$ and $d = 4.587$.

In conclusion, after the experiment, the driver's anger level is expected to decrease. Compared with the AD condition, the anger score under the TTS-RD and AES-RD conditions significantly decreased after the experiment, and the anger returned to the level before the induction of anger. In addition, participants believed that the improvement of AES-RD in anger was more significant.

2) Regulation Success Ratings: The one-way ANOVA showed that in the scores of the regulation success scale, the scores of the AES-RD condition ($M = 7.07$ and $SD = 1.93$) was higher than that of the TTS-RD condition ($M = 5.73$ and $SD = 2.03$), and there was a significant difference between the two groups ($F(1, 58) = 6.792, p = 0.012$, and $\eta_p^2 = 0.105$). The results showed that speech-based regulation is successful for drivers. In addition, participants believed that the recording voice was more successful in regulating driving anger.

C. Physiological Data

Research has shown that anger is associated with asymmetric EEG alpha bands in frontal brain activity [61], and left frontal alpha activation has been found to be associated with the ability to suppress negative emotions spontaneously [62]. As shown in (1), EEG asymmetry was calculated by subtracting the natural log of the left hemisphere alpha power from the natural log of the right hemisphere alpha power for each pair of electrodes [63]. A higher score indicates relatively large left brain activity, while a lower score indicates relatively large right brain activity. Correspondingly, a higher score is considered to have a better regulation effect, and a lower score is considered to be a poorer regulation effect

$$L = \ln\left(P_{\text{right}}\right) - \ln(P_{\text{left}}). \tag{1}$$

1) Straight Driving: In terms of the EEG alpha-band asymmetry in the straight scenario, the analysis results showed that only F3-F4 has a significant difference under the four different driving conditions ($F(3, 112) = 8.616, p < 0.001$, and $\eta_p^2 = 0.188$). On F3-F4 electrodes, post hoc comparisons revealed that there was no statistical difference in the regulation quality between the AES-RD and TTS-RD conditions, but the scores of AES-RD ($M = 0.37$ and $SD = 0.43$) were significantly higher than those of AD ($M = -0.17$ and $SD = 0.52$), $p < 0.001$ and $d = 1.132$; the scores of AES-RD ($M = 0.37$ and $SD = 0.43$) significantly higher than those of ND ($M = 0.18$ and $SD = 0.45$), $p = 0.037$ and $d = 0.845$; the scores of TTS-RD ($M = 0.33$ and $SD = 0.40$) significantly higher than those of AD ($M = -0.17$ and $SD = 0.52$), $p = 0.007$ and $d = 1.078$ (see Table IV). Drivers showed stronger left brain activity under auditory regulation. In addition, although there was no significant difference in EEG asymmetry at Fp1-Fp2, AF-AF4, and F7-F8, on the whole, the scores of auditory regulation were higher than those of the AD and ND conditions. The reason why the difference between F3-F4 is statistically significant may be that F3-F4 corresponds to the auditory functional area of the brain.

As shown in Fig. 6, in the straight scenario, the EEG asymmetry value in F3-F4 under the AES-RD and TTS-RD conditions is significantly higher than that under the AD condition, that is, both AES-RD and TTS-RD have a regulation effect. Although there is no statistical difference in the EEG asymmetry value of F3-F4 between the AES-RD and TTS-RD conditions, the overall score of AES-RD is higher than that of TTS-RD, that is, in the straight scenario, the AES-RD regulation effect has a slight advantage.

2) Obstacle Avoidance: During the obstacle avoidance, the EEG analysis revealed that only F3-F4 has a significant difference under the four different driving conditions ($F(3, 112) = 8.616, p < 0.001$, and $\eta_p^2 = 0.188$). On F3-F4 electrodes, post hoc comparisons revealed that the score of AES-RD ($M = 0.36$ and $SD = 0.48$) was significantly higher than those of TTS-RD ($M = 0.23$ and $SD = 0.37$), $p = 0.019$ and $d = 0.957$; AES-RD ($M = 0.36$ and $SD = 0.48$) significantly higher than those of AD ($M = -0.04$ and $SD = 0.57$), $p = 0.007$ and $d = 1.116$; the scores of AES-RD ($M = 0.37$ and $SD = 0.43$) significantly higher than those of ND ($M = 0.15$ and $SD = 0.25$), $p = 0.026$ and $d = 0.905$; the scores of TTS-RD ($M = 0.23$ and $SD = 0.37$) significantly higher than those of AD ($M = -0.04$ and $SD = 0.57$), $p = 0.007$ and $d = 0.836$. (see Table IV). Drivers showed stronger left brain activity under auditory regulation. In addition, although there was no significant difference in EEG asymmetry at Fp1-Fp2, AF-AF4, and F7-F8, on the whole, the scores of the AES-RD, TTS-RD, and ND conditions were higher than those of the AD condition. The reason why the difference between F3-F4 is statistically significant may be that F3-F4 corresponds to the auditory functional area of the brain.

As shown in Fig. 6, in obstacle avoidance, the EEG asymmetry value in F3-F4 under the AES-RD and TTS-RD conditions is significantly higher than that under the AD condition, that is, both AES-RD and TTS-RD have a regulation effect. Furthermore, the overall score of AES-RD is higher than that of TTS-RD; that is, in the straight scenario, the AES-RD regulation effect has a slight advantage

D. Driving Behavior

Studies have found that anger can negatively impact various measures of driving behavior and increase the risk behaviors of violating traffic signs and signals, speeding, accelerating, and decelerating. In the driving behavior analysis, this article uses average speed, accelerator pedal angle, and brake pedal

TABLE IV
RESULTS OF EEG DATA ANALYSIS AT FOUR DRIVING CONDITIONS

EEG	**AES-RD**	**TTS-RD**	**AD**	**ND**	Cohens'd					
	M (SD)	M (SD)	M (SD)	M (SD)	da	db	dc	dd	de	df
Straight Driving										
Fp2-Fp1	-0.09 (0.73)	-0.02 (0.73)	-0.20 (0.84)	-0.06 (0.57)	0.096	0.140	0.246	0.229	0.161	0.195
AF4-AF3	0.18 (0.40)	0.19 (0.39)	-0.10 (0.77)	-0.02 (0.89)	0.115	0.449	0.748	0.366	0.414	0.194
F4-F3	0.37 (0.43)	0.33 (0.40)	-0.17 (0.52)	0.18 (0.45)	0.296	1.132***	0.845*	1.078**	0.352	0.720**
F8-F7	0.28 (1.02)	0.01 (0.90)	0.29 (0.62)	0.004 (1.01)	0.277	0.112	0.272	0.357	0.101	0.341
Obstacle Avoidance										
Fp2-Fp1	0.001 (0.38)	0.002 (0.75)	0.08 (0.29)	0.06 (0.33)	0.105	0.379	0.166	0.137	0.1	0.189
AF4-AF3	0.06 (1.27)	0.27 (0.51)	0.01 (1.15)	0.21 (0.52)	0.217	0.373	0.25	0.133	0.117	0.186
F4-F3	0.36 (0.48)	0.23 (0.37)	-0.04 (0.57)	0.15 (0.25)	0.957*	1.116**	0.905*	0.836*	0.483	0.708
F8-F7	0.16 (1.01)	0.05 (0.76)	0.27 (0.70)	0.32 (0.62)	0.175	0.127	0.182	0.322	0.472	0.193

da: AES-RD vs. TTS-RD; db: AES-RD vs. AD; dc: AES-RD vs. ND; dd: TTS-RD vs. AD de: TTS-RD vs. ND df: AD vs. ND; *$p < .05$, **$p < .01$, ***$p < .001$.

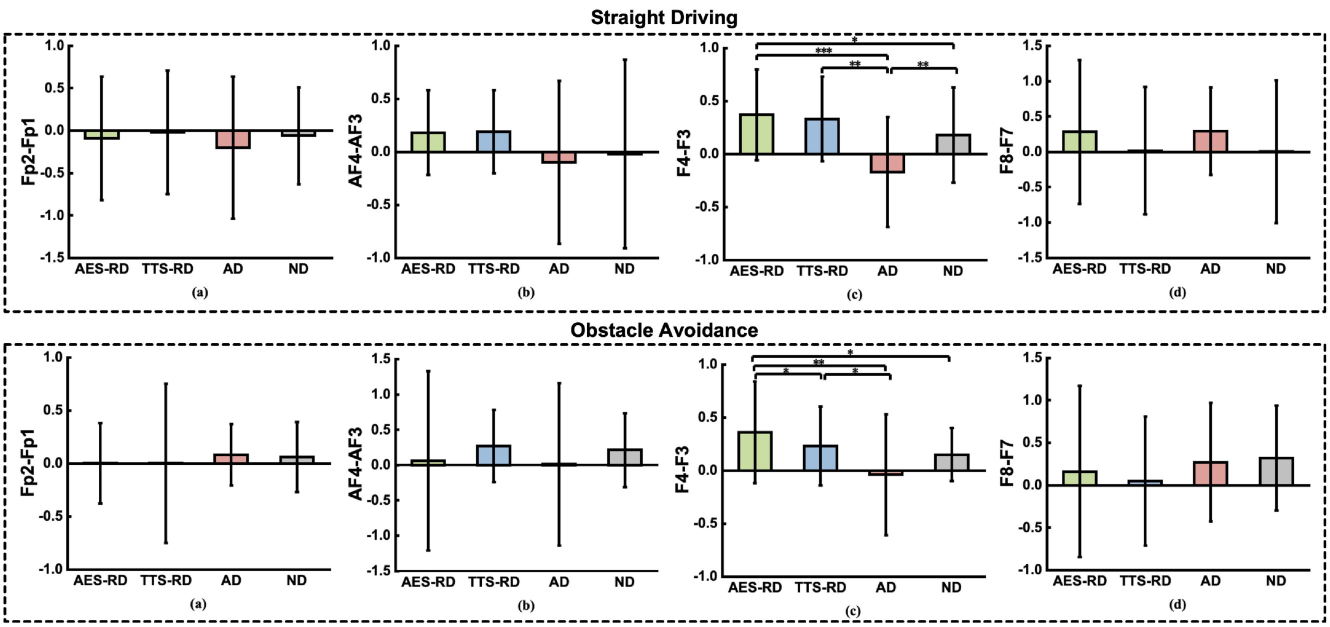

Fig. 6. Comparison of EEG under four driving conditions. Error bars indicate the standard error of the mean. *p < 0.05, **p < 0.01, and ***p < 0.001. (a) Fp2-p1, (b) AF4-AF3, (c) F4-F3, and (d) F8-F7.

force as driving behavior indicators [56], and compares the differences in vehicle longitudinal control under the four driving conditions.

1) Straight Driving: In the straight-driving scenario, the results of one-way ANOVA show that the average speed $F(3, 116) = 5.2, p = 0.002$, and $\eta_p^2 = 0.119$, accelerator $F(3, 116) = 8.808, p < 0.001$, and $\eta_p^2 = 0.186$, brake pedal $F(3, 116) = 7.552, p < 0.001$, and $\eta_p^2 = 0.163$ has significant difference. In terms of average speed, multiple comparison results after the event showed that no significant difference was found between the AES-RD and TTS-RD conditions, but the average speed under the AD condition (M = 24.25 and SD = 2.83) was significantly higher than that under the ND (M = 22.10, SD = 0.98, p = 0.002, and d = 1.015) and AES-RD conditions (M = 22.43, SD = 2.39, p = 0.015, and d = 0.811). For the accelerator pedal angle, no significant difference was found between the AES-RD and TTS-RD conditions, but the pedal depth displayed under the TTS-RD condition (M = 36.96 and SD = 16.13) was significantly lower than that under the AD condition (M = 53.97 and SD = 20.25) $p < 0.001$ and d = 1.789; the pedal depth under the AES-RD condition (M = 33.79 and SD = 11.78) is significantly lower than that under the AD condition (M = 53.97 and SD = 20.25), $p < 0.001$ and d = 2.238; the pedal depth under the ND condition (M = 37.17 and SD = 18.45) is significantly lower than that under the AD condition (M = 53.97 and SD = 20.25), $p < 0.001$ and d = 1.993; for brake pedal force, the pressure under the AES-RD condition (M = 22.08 and SD = 12.50) is significantly lower than that under the TTS-RD condition (M = 27.30, SD = 15.32), p = 0.044 and d = 0.784; the pressure under the TTS-RD condition (M = 27.30 and SD = 15.32) is significantly lower than that under the AD condition (M = 39.49 and SD = 23.08), p = 0.004 and d = 1.156; the pressure under the AES-RD (M = 22.08 and SD = 12.50) is significantly lower than that under the AD condition (M = 39.49 and SD = 23.08), $p < 0.001$ and d = 1.792; the pressure under the ND condition (M = 22.06 and SD = 12.21) is significantly lower than that under the AD condition (M = 39.49 and SD = 23.08), $p < 0.001$ and d = 1.623 (see Table V and Fig. 7).

TABLE V
RESULTS OF DRIVING BEHAVIOR FOR FOUR DRIVING CONDITIONS

Driving Behavior	AES-RD	TTS-RD	AD	ND	Cohens'd					
	M (SD)	M (SD)	M (SD)	M (SD)	da	db	dc	dd	de	df
Straight Driving										
Average speed (m/s)	22.43 (2.39)	22.93 (2.19)	24.25 (2.83)	22.10 (0.98)	0.258	0.811*	0.207	0.571	0.526	1.015**
Mean gas position (°)	33.79 (11.78)	36.96 (16.13)	53.97 (20.25)	37.17 (18.45)	0.371	2.238***	0.354	1.789***	0.026	1.993***
Mean brake force (N)	22.08 (12.50)	27.30 (15.32)	39.49 (23.08)	22.06 (12.21)	0.784*	1.792 ***	0.003	1.156**	0.728	1.623***
Obstacle Avoidance										
Average speed (m/s)	14.42 (2.23)	15.09 (2.80)	17.31 (3.78)	14.07 (2.73)	0.871*	1.831***	0.573	2.199***	0.236	1.668***
Mean gas position (°)	4.13 (3.16)	4.85 (4.40)	5.40 (5.30)	3.80 (2.60)	0.282	0.414	0.178	0.152	0.465	0.701
Mean brake force (N)	6.07 (7.78)	7.81 (10.32)	9.75 (12.42)	5.33 (5.61)	0.995*	0.798*	0.206	0.502	0.545	0.836*

da: AES-RD vs. TTS-RD; db: AES-RD vs. AD; dc: AES-RD vs. ND; dd: TTS-RD vs. AD de: TTS-RD vs. ND df: AD vs. ND; $*p < .05$, $**p < .01$, $***p < .001$.

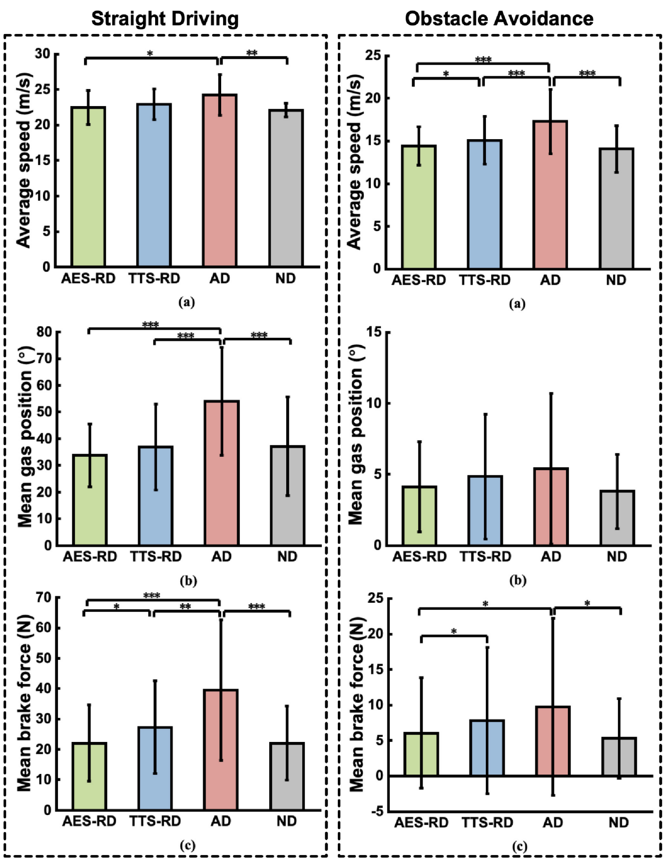

Fig. 7. Comparison of driving behavior under four driving conditions. Error bars indicate the standard error of the mean. $*p < 0.05$, $**p < 0.01$, and $***p < 0.001$. (a) Average speed, (b) mean gas position, and (c) mean brake force.

In a word, in the straight-driving scenario, both AES-RD and TTS-RD interventions positively affect the regulation quality of the driver's anger, especially on the driving behavior. After auditory regulation, the driver's driving performance is significantly improved. Although there is no statistical difference in average speed and accelerator pedal angle between the two auditory regulations, on the whole, the average speed and accelerator pedal angle of the AES-RD condition are both smaller than those of the TTS-RD condition. That is, the AES-RD regulation effect is more favorable in the straight-driving scenario.

2) Obstacle Avoidance: In obstacle avoidance, a one-way ANOVA indicates that there are significant differences in the average speed ($F(3, 116) = 7.304$, $p < 0.001$, and $\eta_p^2 = 0.159$) and brake pedal force ($F(3, 116) = 7.3$, $p < 0.001$, and $\eta_p^2 = 0.159$).

In terms of average speed, the results of multiple post hoc comparisons showed that the average speed in AD conditions ($M = 17.31$ and $SD = 3.78$) was significantly higher than that in ND conditions ($M = 14.07$, $SD = 2.73$, $p < 0.001$, and $d = 1.668$), under TTS-RD conditions ($M = 15.09$, $SD = 2.80$, $p < 0.001$, and $d = 2.199$) and under AES-RD conditions ($M = 14.42$, $SD = 2.23$, $p < 0.001$, and $d = 1.831$). The average speed in the AES-RD condition ($M = 14.42$ and $SD = 2.23$) was slightly lower than that in the TTS-RD condition ($M = 15.09$, $SD = 2.80$, $p = 0.026$, and $d = 0.871$). For brake pedal force, although no significant difference was found between TTS-RD and AD, the pressure in the AES-RD ($M = 6.07$ and $SD = 7.78$) condition was slightly less than that in the TTS-RD condition ($M = 7.81$ and $SD = 10.32$), $p = 0.015$ and $d = 0.995$; the pressure in the AES-RD ($M = 6.07$ and $SD = 7.78$) condition was significantly less than the AD condition ($M = 9.75$ and $SD = 12.42$), $p = 0.048$ and $d = 0.798$; the pressure in the ND ($M = 22.06$ and $SD = 12.21$) condition was significantly smaller than that in the AD condition ($M = 39.49$ and $SD = 23.08$), $p < 0.001$, and $d = 1.623$, (see Table V and Fig. 7).

To sum up, in the obstacle avoidance scenario, both AES-RD and TTS-RD interventions have a positive impact on the driver's anger regulation, especially on driving behavior. After auditory regulation, the driver's driving behavior is milder, and the average speed and brake pedal force are smaller. On the whole, the AES-RD regulation has more advantages. It is worth noting that there is no statistical difference in the accelerator pedal angle between the AES-RD and TTS-RD conditions, which may be that acceleration is not required during the obstacle avoidance scenario.

E. Driving Risk

To evaluate the trajectory safety of the drivers under different conditions from the perspective of driving risk, the artificial potential field (APF) method is adopted to derive the diving risk quantitatively. As a typical numerical representation approach, the APF together with its varieties has been proven to be effective in various kinds of scenarios [64]. The surrounding vehicles, lane boundaries, and other uncrossable positions will be represented by peaks with different heights in APF. Thus, the higher the peak in APF is, the greater the risk will be.

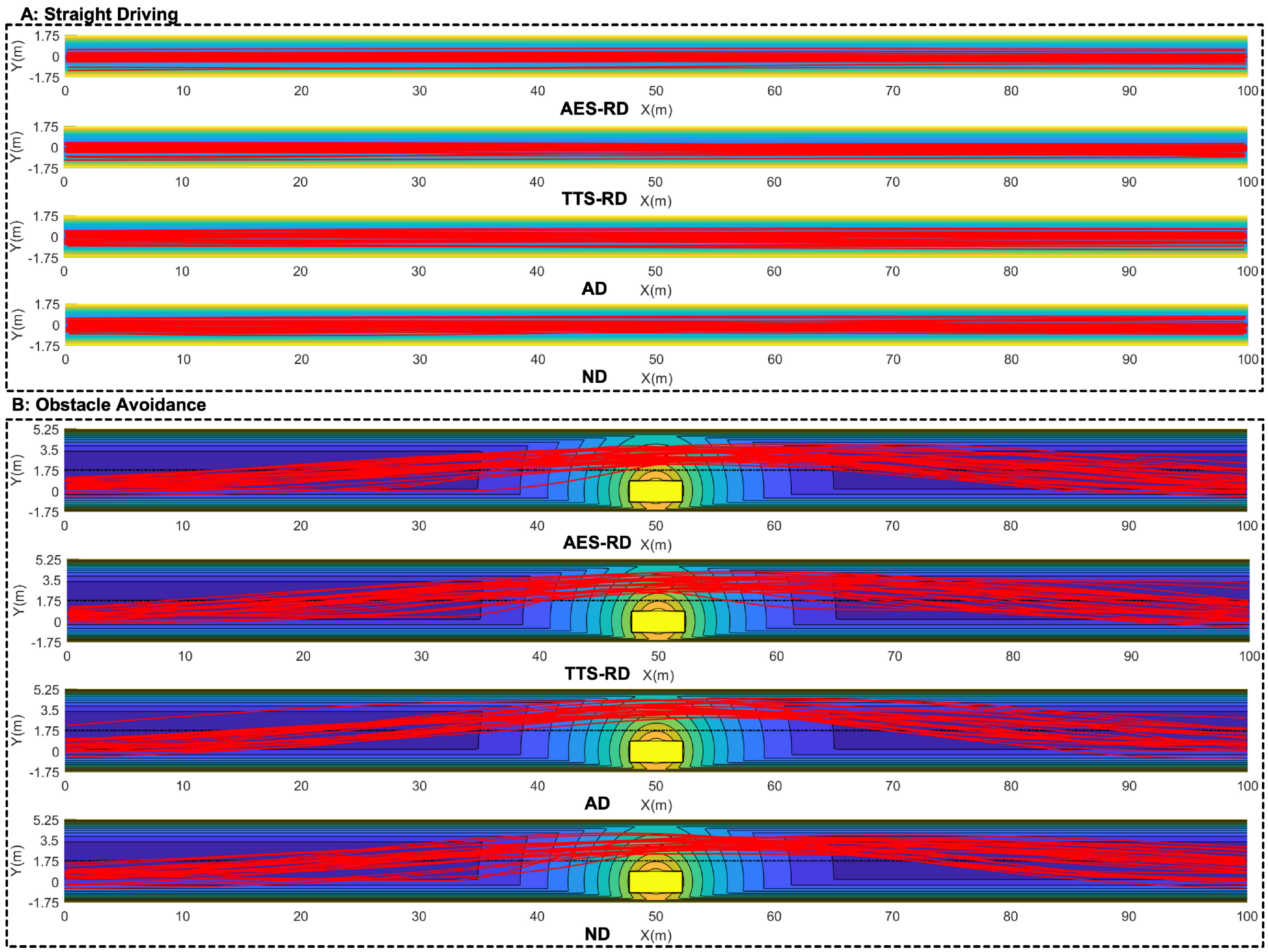

Fig. 8. Mapping of trajectories on corresponding APF.

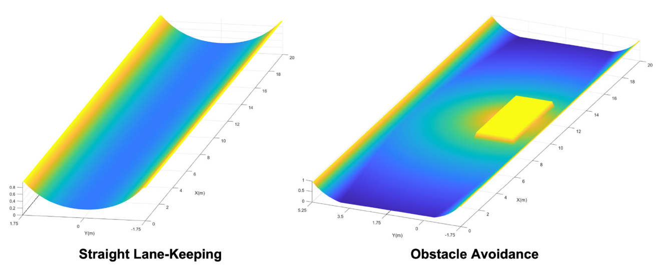

Fig. 9. APF established of different conditions.

In this section, the risk in APF of two conditions, including straight lane-keeping and obstacle avoidance will be analyzed and discussed. First, the APF in straight lane-keeping is established considering only the lane boundaries, as shown in Figs. 8 and 9. The risk function of lane or road boundary is constructed with the exponential formula given in (2). According to the exponential function characteristics, the punishment will be amplified exponentially when the ego vehicle is close to the uncrossable area, in an ideal way

$$U_1 = e^{(-K_{\text{rate1}}|Y-Y_{\max}|-D_b)} + e^{(-K_{\text{rate1}}|Y-Y_{\min}|-D_b)}. \tag{2}$$

Then, the APF in obstacle avoidance conditions considering the road boundary and the obstacle vehicle is established as shown in Fig. 9. Besides the boundary collision risk function in (3), another exponential risk function representing the obstacle vehicle is constructed as (4). The difference is that the occupation of the vehicle body is considered. Finally, the maximum of $U1$ and $U2$ is treated as the comprehensive driving risk in obstacle avoidance conditions

$$U_2 = \begin{cases} e^{D_r}, & \text{if } X \in D_{\text{occupation}} \\ e^{-\left(K_{\text{rate2}}\sqrt{(X-X_b)^2+(Y-Y_b)^2}-D_r\right)}, & \text{else} \end{cases} \tag{3}$$

$$U = \max(U_1, U_2). \tag{4}$$

In these risk functions, K_{rate1} and K_{rate2} are the gradient coefficients and are set to be 1.2 and 0.15, respectively. While D_b and D_r are the peak coefficients which are set be zero here. $Y_{\max}$ and $Y_{\min}$ are the upper and lower boundaries of the road or lane. A road with two lanes is configured in this study and the lane width is set as 3.5 m. The original point of the coordinate system is located at the ideal starting point of the tested vehicle. (X, Y) and (X_b, Y_b) are the coordinates of ego vehicle and obstacle, respectively, while $D_{\text{occupation}}$ refers to the area occupied by the vehicle body. Next, the vehicle trajectories will be mapped onto the corresponding APF and the risk can be obtained with the aforementioned risk function (see Fig. 8).

1) Straight Driving: In the straight-driving scenario, the one-way ANOVA results observed that there was no significant

TABLE VI
RESULTS OF DRIVING RISK FOR FOUR DRIVING CONDITIONS

Driving Risk	AES-RD	TTS-RD	AD	ND	Cohens'd					
	M (SD)	M (SD)	M (SD)	M (SD)	da	db	dc	dd	de	df
Straight Driving										
Average risk	0.272(0.048)	0.271(0.042)	0.278(0.042)	0.271(0.027)	0.027	0.285	0.029	0.249	0.007	0.275
Obstacle Avoidance										
Average risk	0.180(0.021)	0.179(0.034)	0.196(0.029)	0.179(0.034)	0.087	0.965*	0.087	0.827*	0.029	0.827*

da: AES-RD vs. TTS-RD; db: AES-RD vs. AD; dc: AES-RD vs. ND; dd: TTS-RD vs. AD de: TTS-RD vs. ND df: AD vs. ND; $*p < .05$, $**p < .01$, $***p < .001$.

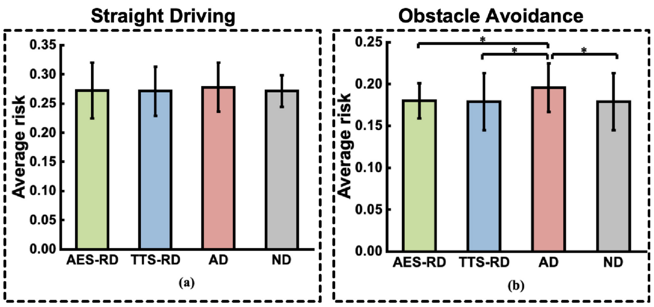

Fig. 10. Comparison of driving risk under four driving conditions. Error bars indicate standard error of the mean. $*p < 0.05$, $**p < 0.01$, $***p < 0.001$.

difference in the average driving risk under the four conditions, $F(3, 107) = 0.174, p = 0.914$, and $\eta_p^2 = 0.006$. The paired t-test showed that although there was no significant difference among the average driving risk under the AES-RD, TTS-RD, and AD conditions, the average driving risk under the AD condition was slightly higher than that under the AES-RD and TTS-RD conditions (see Table VI and Fig. 10). In conclusion, in the straight road, both AES-RD and TTS-RD have a certain effect on the average driving risk of drivers. Although the average driving risk under auditory regulation was not significantly different from that under AD, the average driving risk under the AES-RD and TTS-RD conditions was overall smaller.

2) Obstacle Avoidance: In the obstacle avoidance, the one-way ANOVA results found that there was no significant difference in the average driving risk under the four conditions, $F(3, 107) = 1.847, p = 0.143$, and $\eta_p^2 = 9.053$. The paired t-test showed that although no significant difference was found in the average driving risk between the AES-RD condition and the TTS-RD condition, the average driving under the AD condition ($M = 0.196$ and $SD = 0.029$) was significantly higher than that under the AES-RD ($M = 0.180$, $SD = 0.021$, $p = 0.024$, and $d = 0.965$) and TTS-RD ($M = 0.179$, $SD = 0.034$, $p = 0.049$, and $d = 0.827$) conditions (see Table VI and Fig. 10). In conclusion, in obstacle avoidance, both AES-RD and TTS-RD regulations have a certain effect on the average driving risk of drivers. Although the average driving risk under auditory regulation was not significantly different from that under anger condition, the average driving risk under the AES-RD and TTS-RD conditions was overall smaller.

F. Discussion

Compared with visual regulation, olfactory regulation and tactile regulation, auditory regulation has the following advantages. The auditory regulation is a high-resolution modality that can send complex information quickly through auditory icons (naturally occurring sounds) and earcons (e.g., short tunes or bells), and spearcons (speech-based earcons). Second, auditory regulation conveys directional (spatial) information, and auditory cues can be received from any direction. Third, compared to visual regulation, it reduces mental and visual distractions. Therefore, many studies on auditory emotion regulation have been carried out, including adaptive music, auditory intervention, and empathetic speech. Empathetic speech can adapt to the emotional state of drivers and passengers in the driving environment compared with adaptive music and auditory interventions. Previous research has shown that empathetic speech was not only liked by drivers but also could decrease the impact of sadness and anger on driving.

However, how to design the content description of empathetic speech auditory materials has been one of the contents that has attracted much attention. In this study, we used the emotion regulation strategy based on attention deployment. Combined with the experimental results of in-depth interviews, a reminder style tells the driver about the current road environment (e.g., "there is an obstacle ahead, we need to be careful"). Moreover, the voice content uses positive comments (e.g., "you're driving well") to praise the driver. Moreover, for the question of how to quantitatively analyze and compare the emotion regulation quality, in this study, we used subjective scales, physiological changes (EEG), driving performance, and driving risk to verify the quality of anger regulation in AES and TTS. Notably, since driving scenarios are also closely related to negative emotions generation such as driver anger, we also verified the quality of driver anger regulation in two typical scenarios of straight driving and obstacle avoidance and discussed them separately.

The results show that, compared with unregulated AD, both AES and TTS exhibit excellent driver anger regulation quality in both straight driving and obstacle avoidance scenarios. Specifically, after AES and TTS regulation, drivers performed significantly lower levels of anger, greater left-brain prefrontal activity, more robust driving behavior, and lower driving risks. In addition, AES showed significantly better regulation quality than TTS on some indicators of driver subjective feeling, prefrontal lobe activity, and driving behavior. At the same time, although there is no statistical significance, in both straight driving and obstacle avoidance scenarios, TTS shows a slightly lower driving risk than AES. This may be because AES is the speech recorded by friends, and drivers tend to have more interaction with the AES, which leads to potential distraction and affects the performance of driving tasks.

Further research can focus on the following questions. First, for auditory regulation, the trigger time and duration of the regulation material need further attention. Second, various regulation methods, such as visual regulation, tactile regulation, and olfactory regulation and their mutual integration promoted by technologies, such as metaverse, digital twins, and brain-computer interface [65] are also one of the future directions. Furthermore, the multimodal human–machine interaction regulation also requires the intelligent cockpit to accurately identify the state of humans and comprehensive driving scenario perception. Finally, integrating human emotion recognition and regulation and automated driving system perception [66], decision making [67], and control [68] will also be one of the main directions for intelligent cockpit.

V. Conclusion

This study is proposed the intelligent cockpit composition framework for connected automated driving in the metaverse. The framework includes three layers of perception, cognition and decision, and interaction, and we also discussed the typical technologies in each layer. Meanwhile, we also describe the relationship between the intelligent cockpit framework and the outside environment. The framework can dynamically perceive and understand humans, and provide feedback on the understanding results, which is beneficial to provide a safe, efficient, and enjoyable experience for humans in the intelligent cockpit. In the cognition and decision layers of the proposed framework, we design a case study of active empathetic auditory regulation of driver anger, focusing on improving road traffic safety. We conducted an in-depth interview experiment and designed two auditory regulation materials of active empathy speech and TTS speech. Next, 30 participants were recruited, and they completed a total of 240 anger-regulated driving experiments in the straight and obstacle avoidance scenarios. Finally, we quantitatively analyzed and compared the participants' subjective feelings, physiological changes, driving behaviors, and driving risks, and finally validated the driver anger regulation quality of AES and TTS. The proposed research methods results are beneficial to the design of future intelligent cockpit emotion regulation systems, toward a better intelligent cockpit.

References

[1] F.-Y. Wang, "Metavehicles in the metaverse: Moving to a new phase for intelligent vehicles and smart mobility," *IEEE Trans. Intell. Vehicles*, vol. 7, no. 1, pp. 1–5, Mar. 2022.

[2] L. Li et al., "Parallel testing of vehicle intelligence via virtual-real interaction," *Sci. Robot.*, vol. 4, no. 28, 2019, Art. no. eaaw4106.

[3] X. Wang, X. Zheng, W. Chen, and F.-Y. Wang, "Visual human–Computer interactions for intelligent vehicles and intelligent transportation systems: The state of the art and future directions," *IEEE Trans. Syst., Man, Cybern., Syst.*, vol. 51, no. 1, pp. 253–265, Jan. 2021.

[4] F.-Y. Wang, Y. Li, W. Zhang, G. Bennett, and N. Chen, "Digital twin and parallel intelligence based on location and transportation: A vision for new synergy between the IEEE crfid and itss in cyberphysical social systems [society news]," *IEEE Intell. Transp. Syst. Mag.*, vol. 13, no. 1, pp. 249–252, Mar. 2021.

[5] R. Tan et al., "Xsickness in intelligent mobile spaces and metaverses," *IEEE Intell. Syst.*, vol. 37, no. 5, pp. 86–94, Sep./Oct. 2022.

[6] Y. Ma, Z. Wang, H. Yang, and L. Yang, "Artificial intelligence applications in the development of autonomous vehicles: A survey," *IEEE/CAA J. Automatica Sinica*, vol. 7, no. 2, pp. 315–329, Mar. 2020.

[7] D. Cao et al., "Future directions of intelligent vehicles: Potentials, possibilities, and perspectives," *IEEE Trans. Intell. Vehicles*, vol. 7, no. 1, pp. 7–10, Mar. 2022.

[8] M. Wu, W. Su, L. Chen, Z. Liu, W. Cao, and K. Hirota, "Weight-adapted convolution neural network for facial expression recognition in human–Robot interaction," *IEEE Trans. Syst., Man, Cybern., Syst.*, vol. 51, no. 3, pp. 1473–1484, Mar. 2021.

[9] X. Huang, W. Wu, and H. Qiao, "Connecting model-based and model-free control with emotion modulation in learning systems," *IEEE Trans. Syst., Man, Cybern., Syst.*, vol. 51, no. 8, pp. 4624–4638, Aug. 2021.

[10] W. Li et al., "A multimodal psychological, physiological and behavioural dataset for human emotions in driving tasks," *Sci. Data*, vol. 9, no. 1, pp. 1–20, 2022.

[11] M. Al-Sharman et al., "A sensorless state estimation for a safety-oriented cyber-physical system in urban driving: Deep learning approach," *IEEE/CAA J. Automatica Sinica*, vol. 8, no. 1, pp. 169–178, Jan. 2021.

[12] O. Schumann, J. Lombacher, M. Hahn, C. Wöhler, and J. Dickmann, "Scene understanding with automotive radar," *IEEE Trans. Intell. Vehicles*, vol. 5, no. 2, pp. 188–203, Jun. 2020.

[13] Z. Shen, A. Elibol, and N. Y. Chong, "Understanding nonverbal communication cues of human personality traits in human-robot interaction," *IEEE/CAA J. Automatica Sinica*, vol. 7, no. 6, pp. 1465–1477, Nov. 2020.

[14] C. Wang, F. Li, Y. Wang, and J. R. Wagner, "Haptic Assistive control with learning-based driver intent recognition for semi-autonomous vehicles," *IEEE Trans. Intell. Vehicles*, early access, Dec. 23, 2021, doi: 10.1109/TIV.2021.3137805.

[15] D. Xiong, D. Zhang, X. Zhao, and Y. Zhao, "Deep learning for EMG-based human-machine interaction: A review," *IEEE/CAA J. Automatica Sinica*, vol. 8, no. 3, pp. 512–533, Mar. 2021.

[16] S. Issa, Q. Peng, and X. You, "Emotion classification using EEG brain signals and the broad learning system," *IEEE Trans. Syst., Man, Cybern., Syst.*, vol. 51, no. 12, pp. 7382–7391, Dec. 2021.

[17] A. O. Akmandor, X. Dai, and N. K. Jha, "YSUY: Your smartphone understands you—Using machine learning to address fundamental human needs," *IEEE Trans. Syst., Man, Cybern., Syst.*, vol. 51, no. 12, pp. 7553–7568, Dec. 2021.

[18] C. Zhang and A. Eskandarian, "A survey and tutorial of EEG-based brain monitoring for driver state analysis," *IEEE/CAA J. Automatica Sinica*, vol. 8, no. 7, pp. 1222–1242, Jul. 2021.

[19] L. Guo and Y. Jia, "Inverse model predictive control (IMPC) based modeling and prediction of human-driven vehicles in mixed traffic," *IEEE Trans. Intell. Vehicles*, vol. 6, no. 3, pp. 501–512, Sep. 2021.

[20] N. Deo and M. M. Trivedi, "Looking at the driver/rider in autonomous vehicles to predict take-over readiness," *IEEE Trans. Intell. Vehicles*, vol. 5, no. 1, pp. 41–52, Mar. 2020.

[21] W. Wang et al., "Decision-making in driver-automation shared control: A review and perspectives," *IEEE/CAA J. Automatica Sinica*, vol. 7, no. 5, pp. 1289–1307, Sep. 2020.

[22] Y. Yang, Z. Gao, Y. Li, Q. Cai, N. Marwan, and J. Kurths, "A complex network-based broad learning system for detecting driver fatigue from EEG signals," *IEEE Trans. Syst., Man, Cybern., Syst.*, vol. 51, no. 9, pp. 5800–5808, Sep. 2021.

[23] B. Baheti, S. Talbar, and S. Gajre, "Towards computationally efficient and realtime distracted driver detection with mobileVGG network," *IEEE Trans. Intell. Vehicles*, vol. 5, no. 4, pp. 565–574, Dec. 2020.

[24] Z. Yan, K. Yang, Z. Wang, B. Yang, T. Kaizuka, and K. Nakano, "Intention-based lane changing and lane keeping haptic guidance steering system," *IEEE Trans. Intell. Vehicles*, vol. 6, no. 4, pp. 622–633, Dec. 2021.

[25] Z. Wang et al., "Driver behavior modeling using game engine and real vehicle: A learning-based approach," *IEEE Trans. Intell. Vehicles*, vol. 5, no. 4, pp. 738–749, Dec. 2020.

[26] J. Huang, Y. Chen, X. Peng, L. Hu, and D. Cao, "Study on the driving style adaptive vehicle longitudinal control strategy," *IEEE/CAA J. Automatica Sinica*, vol. 7, no. 4, pp. 1107–1115, Jul. 2020.

[27] D. Zhang, G. Feng, Y. Shi, and D. Srinivasan, "Physical safety and cyber security analysis of multi-agent systems: A survey of recent advances," *IEEE/CAA J. Automatica Sinica*, vol. 8, no. 2, pp. 319–333, Feb. 2021.

[28] Y.-D. Lin, E. T.-H. Chu, E. Chang, and Y.-C. Lai, "Smoothed graphic user interaction on smartphones with motion prediction," *IEEE Trans. Syst., Man, Cybern., Syst.*, vol. 50, no. 4, pp. 1429–1441, Apr. 2020.

[29] F. Roche and S. Brandenburg, "Should the urgency of visual-tactile takeover requests match the criticality of takeover situations?" *IEEE Trans. Intell. Vehicles*, vol. 5, no. 2, pp. 306–313, Jul. 2020.

[30] H. Liu, F. Sun, B. Fang, and D. Guo, "Cross-modal zero-shot-learning for tactile object recognition," *IEEE Trans. Syst., Man, Cybern., Syst.*, vol. 50, no. 7, pp. 2466–2474, Jul. 2020.

[31] M. Hasenjäger, M. Heckmann, and H. Wersing, "A survey of personalization for advanced driver assistance systems," *IEEE Trans. Intell. Vehicles*, vol. 5, no. 2, pp. 335–344, Jun. 2020.

[32] P. Shi and B. Yan, "A survey on intelligent control for multiagent systems," *IEEE Trans. Syst., Man, Cybern., Syst.*, vol. 51, no. 1, pp. 161–175, Jan. 2021.

[33] W. Li et al., "Visual-attribute-based emotion regulation of angry driving behaviors," *IEEE Intell. Transp. Syst. Mag.*, vol. 14, no. 3, pp. 10–28, May/Jun. 2022.

[34] L. Chen, M. Wu, M. Zhou, Z. Liu, J. She, and K. Hirota, "Dynamic emotion understanding in human–robot interaction based on two-layer fuzzy SVR-TS model," *IEEE Trans. Syst., Man, Cybern., Syst.*, vol. 50, no. 2, pp. 490–501, Feb. 2020.

[35] X. Sun, Z. Pei, C. Zhang, G. Li, and J. Tao, "Design and analysis of a human–machine interaction system for researching human's dynamic emotion," *IEEE Trans. Syst., Man, Cybern., Syst.*, vol. 51, no. 10, pp. 6111–6121, Oct. 2021.

[36] W. Li et al., "CogEmoNet: A cognitive-feature-augmented driver emotion recognition model for smart cockpit," *IEEE Trans. Comput. Social Syst.*, vol. 9, no. 3, pp. 667–678, Jun. 2022.

[37] J. J. Gross, "Emotion regulation: Current status and future prospects," *Psychol. Inquiry*, vol. 26, no. 1, pp. 1–26, 2015.

[38] B. Donmez, L. N. Boyle, and J. D. Lee, "Differences in off-road glances: Effects on young drivers' performance," *J. Transp. Eng.*, vol. 136, no. 5, pp. 403–409, 2010.

[39] Y. Zhu, Y. Wang, G. Li, and X. Guo, "Recognizing and releasing drivers' negative emotions by using music: Evidence from driver anger," in *Proc. Int. Conf. Autom. User Interfaces Interact. Veh. Appl.*, 2016, pp. 173–178.

[40] S. M. FakhrHosseini and M. Jeon, "How do angry drivers respond to emotional music? A comprehensive perspective on assessing emotion," *J. Multimodal User Interfaces*, vol. 13, no. 2, pp. 137–150, 2019.

[41] S. M. Fakhrhosseini, S. Landry, Y. Y. Tan, S. Bhattarai, and M. Jeon, "If you're angry, turn the music on: Music can mitigate anger effects on driving performance," in *Proc. Int. Conf. Autom. User Interfaces Interact. Veh. Appl.*, 2014, pp. 1–7.

[42] W. Brodsky and M. Kizner, "Exploring an alternative in-car music background designed for driver safety," *Transp. Res. F Traffic Psychol. Behav.*, vol. 15, no. 2, pp. 162–173, 2012.

[43] M. D. Van Der Zwaag, C. Dijksterhuis, D. De Waard, B. L. Mulder, J. H. Westerink, and K. A. Brookhuis, "The influence of music on mood and performance while driving," *Ergonomics*, vol. 55, no. 1, pp. 12–22, 2012.

[44] C. Pêcher, C. Lemercier, and J.-M. Cellier, "Emotions drive attention: Effects on driver's behaviour," *Safety Sci.*, vol. 47, no. 9, pp. 1254–1259, 2009.

[45] M. FakhrHosseini and M. Jeon, "The effects of various music on angry drivers' subjective, behavioral, and physiological states," in *Proc. Int. Conf. Autom. User Interfaces Interact. Veh. Appl.*, 2016, pp. 191–196.

[46] P. E. Paredes et al., "Just breathe: In-car interventions for guided slow breathing," *Proc. ACM Interact. Mobile Wearable Ubiquitous Technol.*, vol. 2, no. 1, pp. 1–23, 2018.

[47] S. Zepf, N. El Haouij, J. Lee, A. Ghandeharioun, J. Hernandez, and R. W. Picard, "Studying Personalized just-in-time auditory breathing guides and potential safety implications during simulated driving," in *Proc. ACM Conf. User Model. Adaptation Pers.*, 2020, pp. 275–283.

[48] C. Nass et al., "Improving automotive safety by pairing driver emotion and car voice emotion," in *Proc. CHI Conf. Hum. Factors Comput. Syst.*, 2005, pp. 1973–1976.

[49] M. Braun, J. Schubert, B. Pfleging, and F. Alt, "Improving driver emotions with affective strategies," *Multimodal Technol. Interact.*, vol. 3, no. 1, p. 21, 2019.

[50] M. Braun, F. Weber, and F. Alt, "Affective automotive user interfaces–Reviewing the state of emotion regulation in the car." 2020. [Online]. Available: https://arxiv.org/abs/2003.13731.

[51] I.-M. Jonsson, M. Zajicek, H. Harris, and C. Nass, "Thank you, i did not see that: In-car speech based information systems for older adults," in *Proc. CHI Extended Abstr. Human Factors Comput. Syst.*, 2005, pp. 1953–1956.

[52] C. Nass, Y. Moon, and N. Green, "Are machines gender neutral? Gender-stereotypic responses to computers with voices," *J. Appl. Soc. Psychol.*, vol. 27, no. 10, pp. 864–876, 1997.

[53] I.-M. Jonsson, "Social and emotional characteristics of speech-based in-vehicle information systems: Impact on attitude and driving behaviour," Ph.D. dissertation, Dept. Comput. Inf. Sci., Linköping Univ., Linköping, Sweden, 2009.

[54] S. Li, T. Zhang, N. Liu, W. Zhang, D. Tao, and Z. Wang, "Drivers' attitudes, preference, and acceptance of in-vehicle anger intervention systems and their relationships to demographic and personality characteristics," *Int. J. Ind. Ergonom.*, vol. 75, Jan. 2020, Art. no. 102899.

[55] I.-M. Jonsson et al., "Don't blame me i am only the driver: Impact of blame attribution on attitudes and attention to driving task," in *Proc. CHI Extended Abstr. Human Factors Comput. Syst.*, 2004, pp. 1219–1222.

[56] S. Li, T. Zhang, W. Zhang, N. Liu, and G. Lyu, "Effects of speech-based intervention with positive comments on reduction of driver's anger state and perceived workload, and improvement of driving performance," *Appl. Ergonom.*, vol. 86, Jul. 2020, Art. no. 103098.

[57] M. Jeon, B. N. Walker, and T. M. Gable, "The effects of social interactions with in-vehicle agents on a driver's anger level, driving performance, situation awareness, and perceived workload," *Appl. Ergonom.*, vol. 50, pp. 185–199, Sep. 2015.

[58] W. Li et al., "A spontaneous driver emotion facial expression (DEFE) dataset for intelligent vehicles: Emotions triggered by video-audio clips in driving scenarios," *IEEE Trans. Affect. Comput.*, early access, Mar. 3, 2021, doi: 10.1109/TAFFC.2021.3063387.

[59] J. J. Gross and O. P. John, "Individual differences in two emotion regulation processes: Implications for affect, relationships, and well-being," *J. Personal. Soc. Psychol.*, vol. 85, no. 2, pp. 348–362, 2003.

[60] Z. Deng et al., "A probabilistic model for driving-style-recognition-enabled driver steering behaviors," *IEEE Trans. Syst., Man, Cybern., Syst.*, vol. 52, no. 3, pp. 1838–1851, Mar. 2022.

[61] A. Brzezicka, J. Kamiński, O. K. Kamińska, D. Wołyńczyk-Gmaj, and G. Sedek, "Frontal EEG alpha band asymmetry as a predictor of reasoning deficiency in depressed people," *Cogn. Emot.*, vol. 31, no. 5, pp. 868–878, 2017.

[62] D. C. Jackson et al., "Now you feel it, now you don't: Frontal brain electrical asymmetry and individual differences in emotion regulation," *Psychol. Sci.*, vol. 14, no. 6, pp. 612–617, 2003.

[63] J. A. Coan and J. J. Allen, "Frontal EEG asymmetry as a moderator and mediator of emotion," *Biol. Psychol.*, vol. 67, nos. 1–2, pp. 7–49, 2004.

[64] C. Wang, Z. Wang, L. Zhang, H. Yu, and D. Cao, "Post-impact motion planning and tracking control for autonomous vehicles," *Chin. J. Mech. Eng.*, vol. 35, no. 1, pp. 1–18, 2022.

[65] J. Zhuang, K. Geng, and G. Yin, "Ensemble learning based brain–Computer interface system for ground vehicle control," *IEEE Trans. Syst., Man, Cybern., Syst.*, vol. 51, no. 9, pp. 5392–5404, Sep. 2021.

[66] Y. Tian, Y. Zhao, Y. Shi, X. Cao, and D.-L. Yu, "The indirect shared steering control under double loop structure of driver and automation," *IEEE/CAA J. Automatica Sinica*, vol. 7, no. 5, pp. 1403–1416, Sep. 2020.

[67] X. Xu, L. Zuo, X. Li, L. Qian, J. Ren, and Z. Sun, "A reinforcement learning approach to autonomous decision making of intelligent vehicles on highways," *IEEE Trans. Syst., Man, Cybern., Syst.*, vol. 50, no. 10, pp. 3884–3897, Oct. 2020.

[68] J. Tan, C. Xu, L. Li, F.-Y. Wang, D. Cao, and L. Li, "Guidance control for parallel parking tasks," *IEEE/CAA J. Automatica Sinica*, vol. 7, no. 1, pp. 301–306, Jan. 2020.

Wenbo Li received the B.S., M.Sc., and Ph.D. degrees in automotive engineering from Chongqing University, Chongqing, China, in 2014, 2017, and 2021, respectively.

From October 2018 to October 2020, he was a visiting Ph.D. student with the Department of Mechanical and Mechatronics Engineering, University of Waterloo, Waterloo, ON, Canada. He is currently a Postdoctoral Research Fellow with Tsinghua University, Beijing, China. His research interests include intelligent vehicle, intelligent cockpit, human emotion and cognition, driver emotion detection and regulation, human–machine interaction, affective computing, and brain–computer interface.

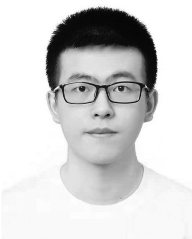

Lei Wu received the B.Sc. degree in automotive engineering from the Hefei University of Technology, Hefei, China, in 2020. He is currently pursuing the M.Sc. degree with the Advanced Manufacturing and Information Technology Laboratory, College of Mechanical and Vehicle Engineering, Chongqing University, Chongqing, China.

His research interests include human–machine interaction, driver anger regulation, and user experience.

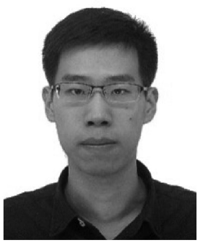

Cong Wang received the B.S. and Ph.D. degrees in automotive engineering from the Beijing Institute of Technology, Beijing, China, in 2016 and 2022, respectively.

He is currently a Postdoctoral Research Fellow with Tsinghua University, Beijing. His research interests mainly include vehicle dynamics and safety control for electric vehicles.

Jiyong Xue received the B.S. degree in automotive engineering from Chongqing University, Chongqing, China, in 2019, where he is currently pursuing the M.Sc. degree with the College of Mechanical and Vehicle Engineering.

His research interests include the modeling of human–machine interaction in intelligent vehicles, speech emotion recognition, and driver emotion regulation.

Wen Hu received the B.S. and M.S. degrees in mechanical engineering from Hunan University, Changsha, China, in 2015 and 2018, respectively, where he is currently pursuing the Ph.D. degree in mechanical engineering with the College of Mechanical and Vehicle Engineering.

He is also a visiting Ph.D. student with the Department of Mechanical and Mechatronics Engineering, University of Waterloo, Waterloo, ON, Canada. His research interests include decision making and trajectory planning, vehicle dynamics, and control in intelligent vehicle.

Shen Li (Member, IEEE) received the Ph.D. degree in transportation engineering from the University of Wisconsin–Madison, Madison, WI, USA, in 2018.

He is a Research Associate with Tsinghua University, Beijing, China. His research is about intelligent transportation systems, architecture design of CAVH system, vehicle-infrastructure cooperative planning and decision method, traffic data mining based on cellular data, and traffic operations and management.

Gang Guo received the B.S., M.S., and Ph.D. degrees in automotive engineering from Chongqing University, Chongqing, China, in 1982, 1984, and 1994, respectively.

He is currently the Chair and the Professor with the Department of Automotive Engineering, Chongqing University, where he also serves as the Associate Director of Chongqing Automotive Collaborative Innovation Center. He has authored and coauthored over 100 refereed journal and conference publications. His research interests include intelligent vehicle, multisense perception, human–machine interaction, brain–computer interface, intelligent manufacturing, and user experience.

Dr. Guo is a Senior Member of the China Mechanical Engineering Society and the Director of the China Automotive Engineering Society. He is also a member of the China User Experience Alliance Committee.

Dongpu Cao (Member, IEEE) received the Ph.D. degree in mechanical engineering from Concordia University, Montreal, QC, Canada, in 2008.

He is the Canada Research Chair of Driver Cognition and Automated Driving, and currently an Associate Professor and the Director of Waterloo Cognitive Autonomous Driving (CogDrive) Lab, University of Waterloo, Waterloo, ON, Canada. He has contributed more than 200 papers and three books. His current research focuses on driver cognition, automated driving, and cognitive autonomous driving.

Dr. Cao received the SAE Arch T. Colwell Merit Award in 2012 and three Best Paper Awards from the ASME and IEEE conferences. He serves as an Associate Editor for IEEE TRANSACTIONS ON VEHICULAR TECHNOLOGY, IEEE TRANSACTIONS ON INTELLIGENT TRANSPORTATION SYSTEMS, IEEE/ASME TRANSACTIONS ON MECHATRONICS, IEEE TRANSACTIONS ON INDUSTRIAL ELECTRONICS, IEEE/CAA JOURNAL OF AUTOMATICA SINICA, and *Journal of Dynamic Systems, Measurement and Control* (ASME). He was a Guest Editor for *Vehicle System Dynamics* and IEEE TRANSACTIONS ON SYSTEMS, MAN, AND CYBERNETICS: SYSTEMS. He serves on the SAE Vehicle Dynamics Standards Committee and acts as the Co-Chair of IEEE ITSS Technical Committee on Cooperative Driving.